Supplementary Information (SI) for Journal of Materials Chemistry A.

Supplementary information

Sulfur-Based Hybrid Multilayers on Li Metal Anodes with Excellent Air Stability for Ultralong-Life and High-Performance Batteries

Chaerim Kim,[a] Seohyun Mun,[a] Jaeyoung Park,[a] Jinho Chang,[a] Boram Cho,[b] Kristian Knemeyer,[b] Andrea Giraldo,[b] Kyeongjae Cho [c] and Myung Mo Sung [a,] *

[a]*Department of Chemistry*
Hanyang University
Seoul 04763, South Korea
E-mail: smm@hanyang.ac.kr

[b]*BASF Schweiz AG*
Basel 4057, Switzerland

[c]*Department of Materials Science and Engineering*
University of Texas at Dallas
Richardson, Texas 75080, USA

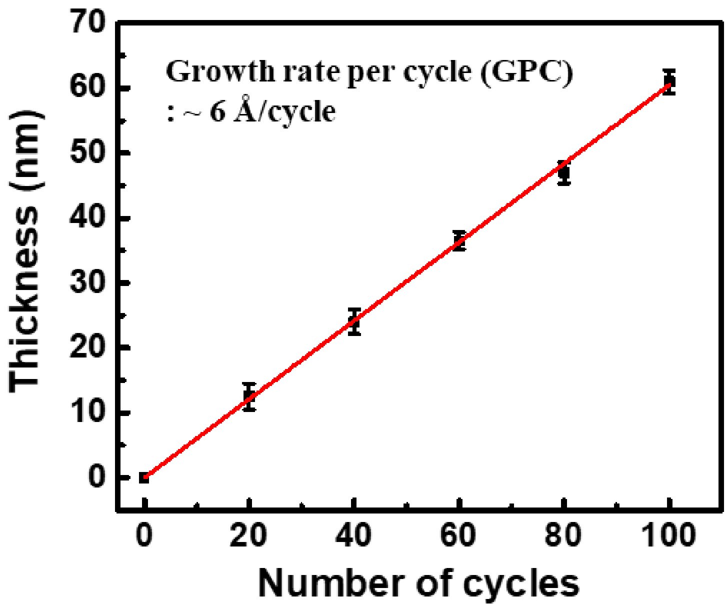

Fig. S1 The film thickness as a function of number of MLD cycles.

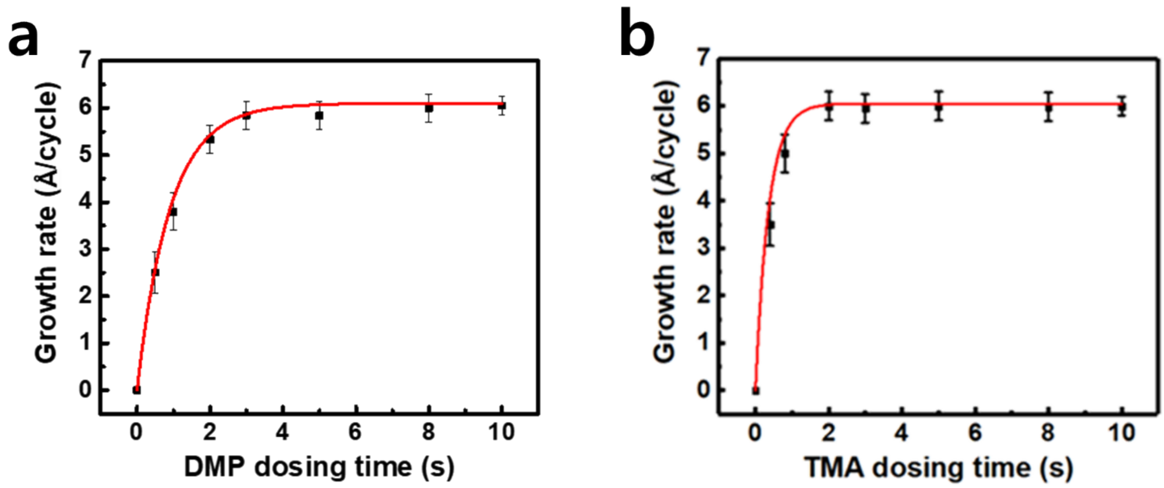

Fig. S2 Growth per cycle (GPC) as a function of DMP dosing time. (a) DMP. (b) TMA.

	Al-DMP@Li				
Element	**Li**	**O**	**C**	**S**	**Al**
Atomic %	0	15.68	41.12	28.39	14.81

Table S1. Atomic percentage of elements detected by XPS analysis of the Al-DMP films.

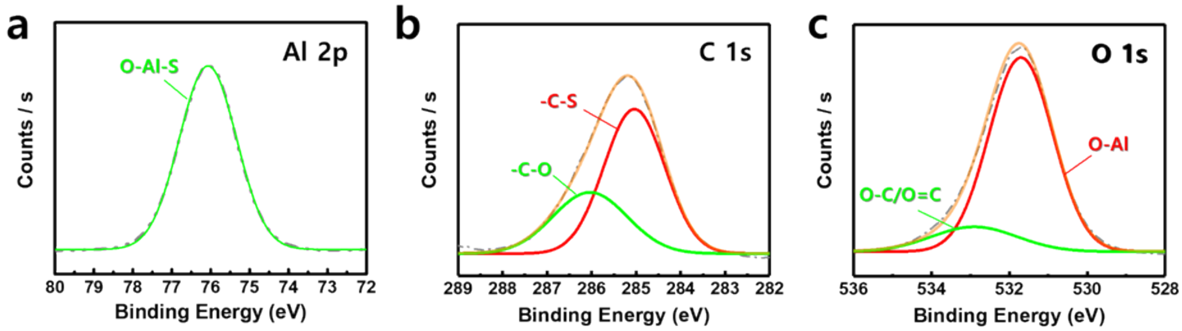

Fig. S3 XP spectra for the Al-DMP multilayer. (a) Aluminum 2p, (b) Carbon 1s, (c) Oxygen 1s.

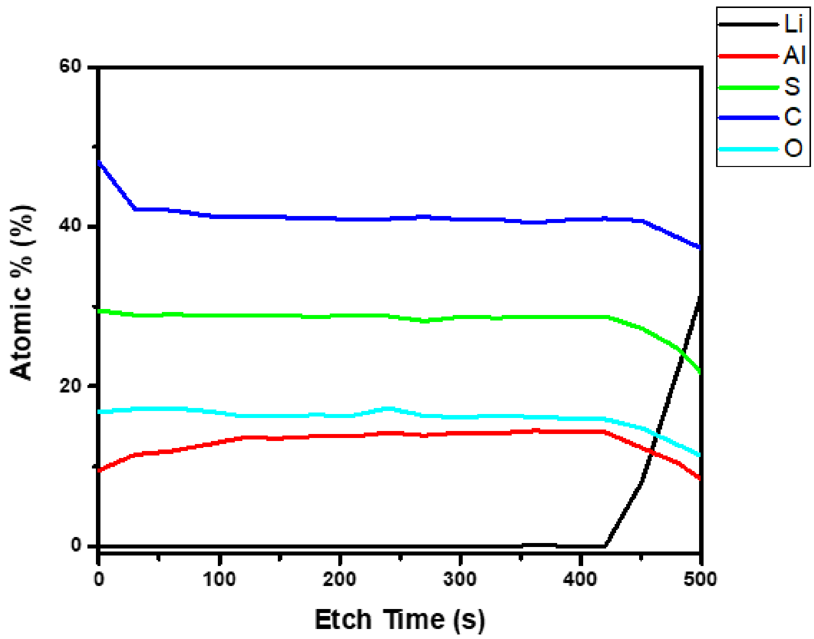

Fig. S4 XPS depth profiling of the Al-DMP multilayer.

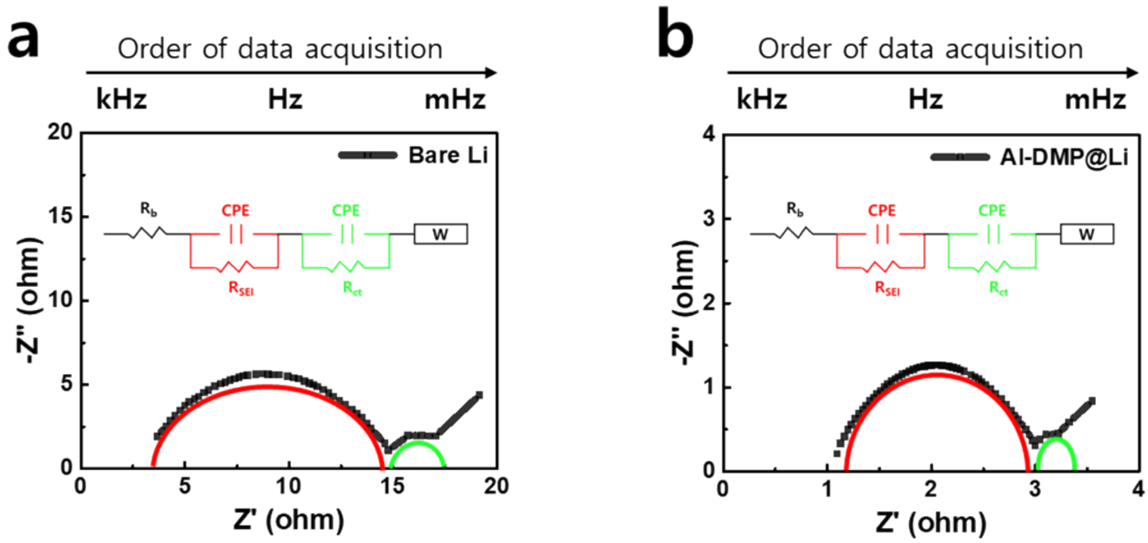

Fig. S5 The interfacial resistance fitted from equivalent circuit model: in which R_b is the bulk resistance of battery, R_{SEI} is the migration resistance of Li ions through SEI, R_{ct} is the charge transfer resistance, CPE is the constant phase element, and the W is the Warburg element. (a) bare Li and (b) Al-DMP@Li after 1 cycle.

	Al-DMP@Li
After 1 cycling (R_{SEI})	1.7
After 1 cycling (σ, S cm^{-1})	1.9x 10^{-6}
After 500 cycling (R_{SEI})	6.4
After 500 cycling (σ, S cm^{-1})	5.1x 10^{-7}

Table S2. Impedance results of Al-DMP@Li symmetric cells at after 1 cycle and after 500 cycles. Li-ion conductivity of the Al-DMP multilayer can be calculated by using an equation:

$$\sigma = \frac{L}{R_{SEI} \times S}$$

where L is the thickness SEI layer (50 nm), the S is the geometric area of electrode/electrolyte interface and the R_{SEI} is obtained from the Nyquist plot.

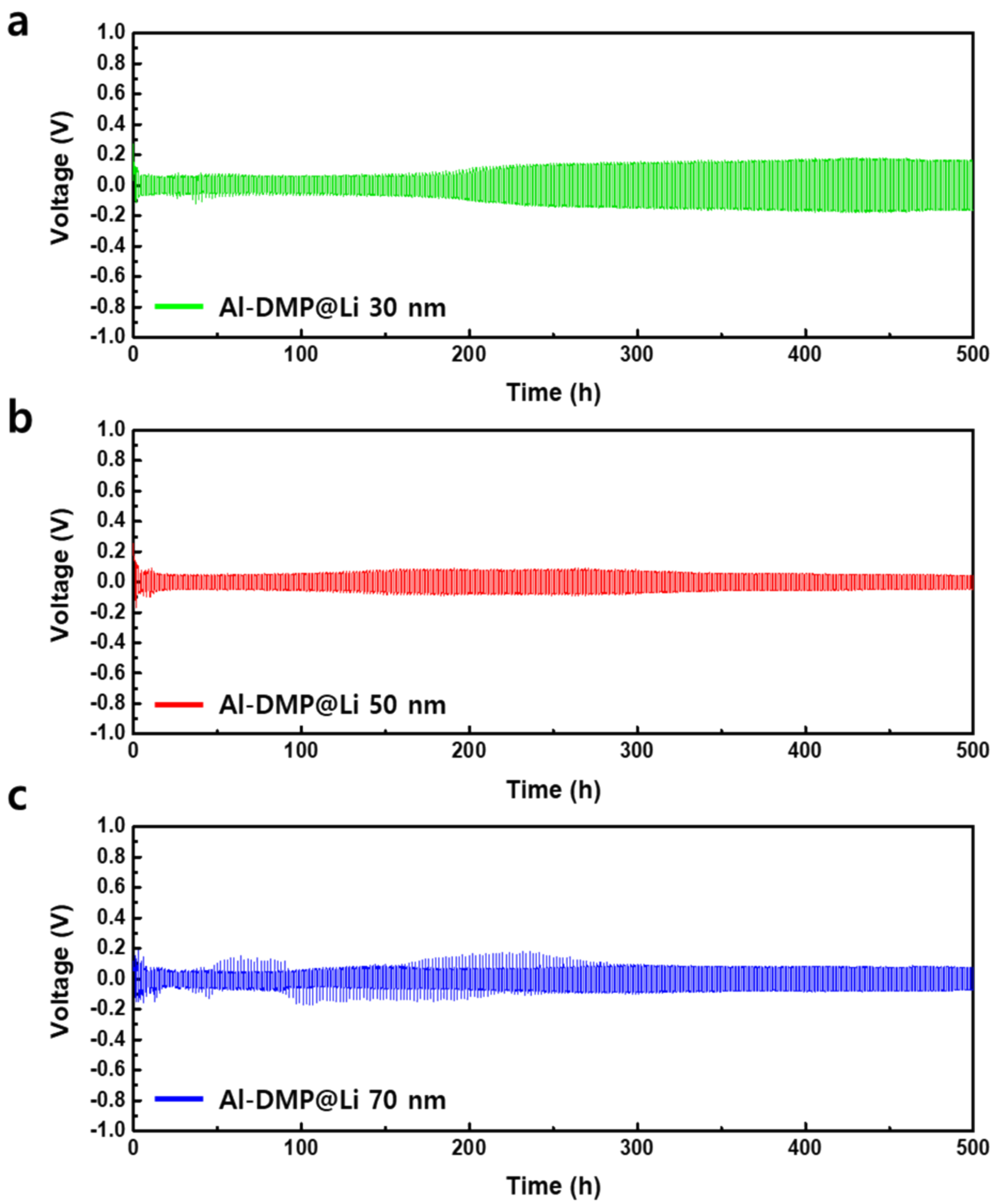

Fig. S6 A comparison of electrochemical performance from various film thickness on Al-DMP multilayers. Galvanostatic cycling performance of Al-DMP@Li symmetric cells at current density/areal capacity of 10 mA cm^{-2}/10 mAh cm^{-2} (a) 30 nm (b) 50 nm (c) 70 nm of Al-DMP.

a

No.	Age [h:m:s:ms]	Theta(M)[deg]	Vol [ul]	Area [mm*2]	BD [mm]
0-0	00:02:57:595	41.2	720.4 pl	59817.24	0.262
0-1	00:02:58:595	41.1	718.3 pl	59846.56	0.262
0-2	00:02:59:595	41.1	718 pl	59879.44	0.263
0-3	00:03:00:595	40.9	714.2 pl	59901.54	0.263
0-4	00:03:01:595	40.9	715.3 pl	59908.54	0.263
0-5	00:03:02:595	40.9	712.2 pl	59892.55	0.263
0-6	00:03:03:595	40.7	709.5 pl	59930.19	0.263
0-7	00:03:04:596	40.7	708.6 pl	59886.91	0.263
0-8	00:03:05:596	40.7	706.6 pl	59887.92	0.263
0-9	00:03:06:596	40.6	704.3 pl	59893.96	0.263
0-10	00:03:07:596	40.6	705.1 pl	59890.84	0.263
0-11	00:03:08:596	40.5	703.3 pl	59893.21	0.263
0-12	00:03:09:596	40.4	701.4 pl	59919.48	0.263
0-13	00:03:10:596	40.4	700.1 pl	59916.07	0.263
0-14	00:03:11:596	40.4	699.3 pl	59877.97	0.263
0-15	00:03:12:596	40.3	696.7 pl	59874.89	0.263
0-16	00:03:13:596	40.3	695.3 pl	59871.38	0.263
0-17	00:03:14:597	40.2	693.8 pl	59860.68	0.263
0-18	00:03:15:597	40.2	693.7 pl	59916.57	0.263
0-19	00:03:16:597	40.1	692.1 pl	59873.52	0.263
0-20	00:03:17:597	40.1	691.9 pl	59901.7	0.263

b

No.	Age [h:m:s:ms]	Theta(M)[deg]	Vol [ul]	Area [mm*2]	BD [mm]
0-0	00:12:06:817	7.8	708.7 pl	103837.2	0.363
0-1	00:12:07:818	7.7	641.1 pl	98381.23	0.353
0-2	00:12:08:817	6.9	617.7 pl	102086.81	0.36
0-3	00:12:09:817	6.4	564.5 pl	100671.13	0.357
0-4	00:12:10:827	5.7	532.1 pl	103543.31	0.363
0-5	00:12:11:817	5	477.7 pl	103568.98	0.363
0-6	00:12:12:817	4.3	422.5 pl	104049.27	0.364
0-7	00:12:13:827	3.5	355.4 pl	103653.18	0.363
0-8	00:12:14:818	3.2	231.7 pl	82400.47	0.324
0-9	00:12:15:817	3	108.1 pl	82100.27	0.318

Table S3. Dynamic contact angle variation with time on (a) bare Li (b) Al-DMP@Li.

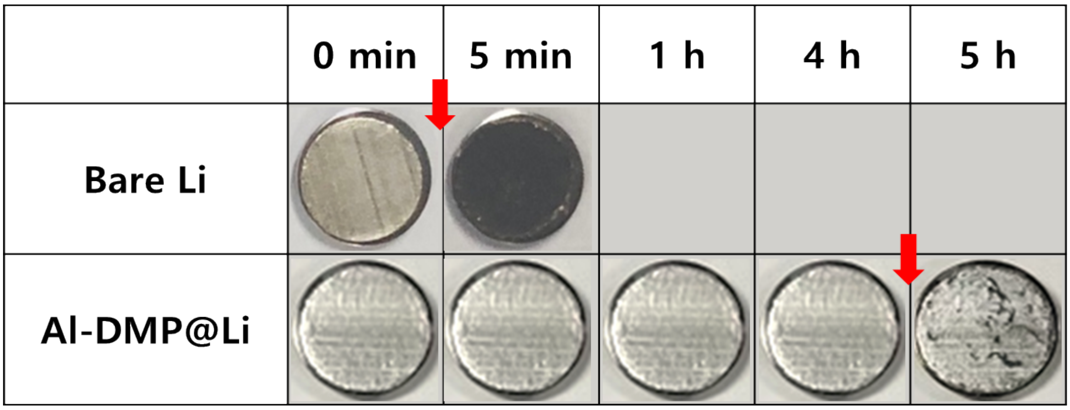

Fig. S7 Digital images of bare Li and Al-DMP@Li exposed to air at 25 °C and 50 % humidity.

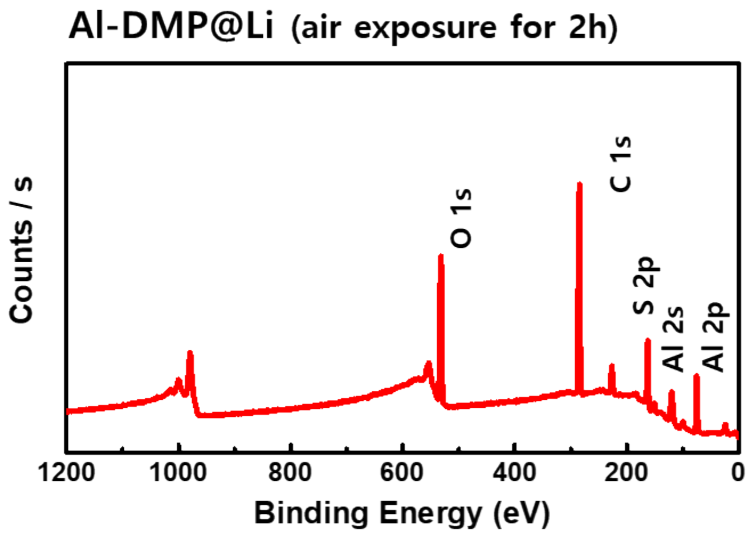

	Al-DMP@Li (air exposure for 1h)				
Element	Li	O	C	S	Al
Atomic %	0	18.44	41.96	25.53	14.07

Fig. S8 XP spectra for the Al-DMP@Li after air exposure for 2h.

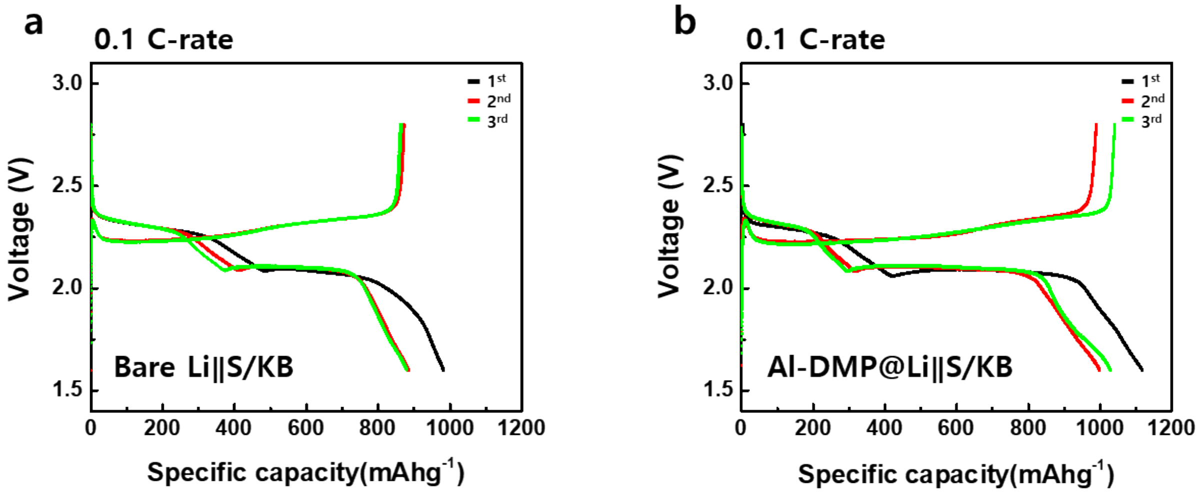

Fig. S9 Voltage profiles of full cells at 0.1 C-rate (a) bare Li‖S/KB (b) Al-DMP@Li‖S/KB.

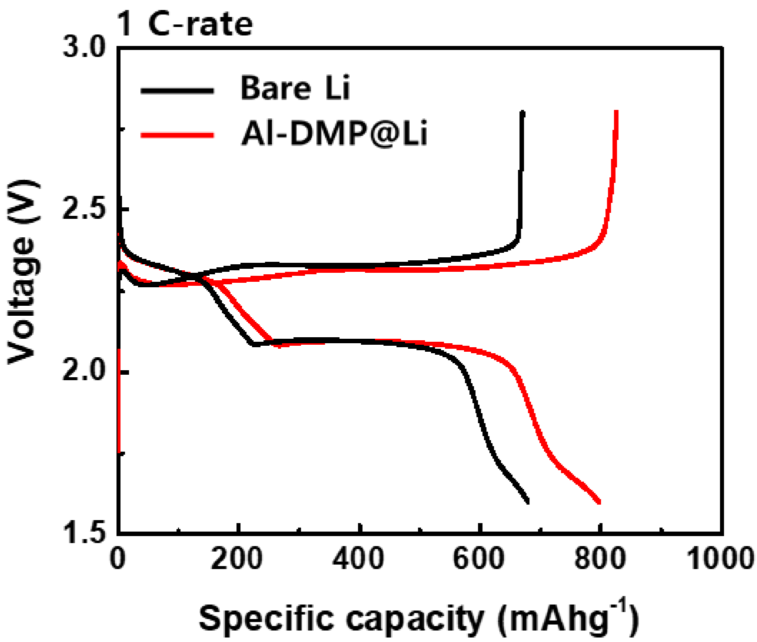

Fig. S10 Voltage profiles of full cells with bare Li‖S/KB and Al-DMP@Li‖S/KB after the 1st charge/discharge.

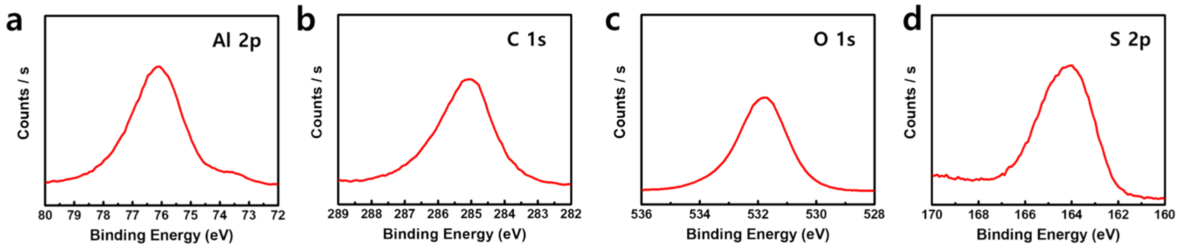

Fig. S11 XP spectra for the Al-DMP multilayer after 100 cycles (a) Aluminum 2p, (b) Carbon 1s, (c) Oxygen 1s, (d) Sulfur 2p.

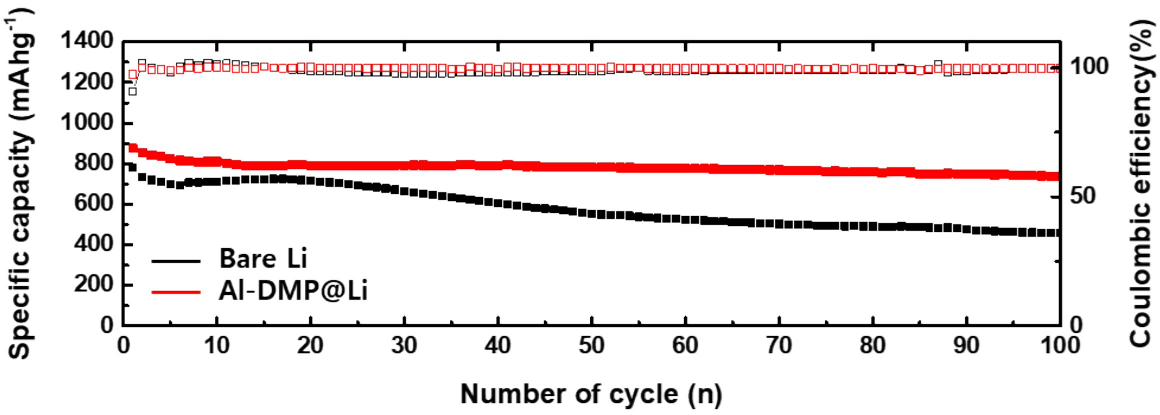

Fig. S12 Electrochemical performance of Li-S full cells with high loading S cathodes (~5 mg cm^{-2}).

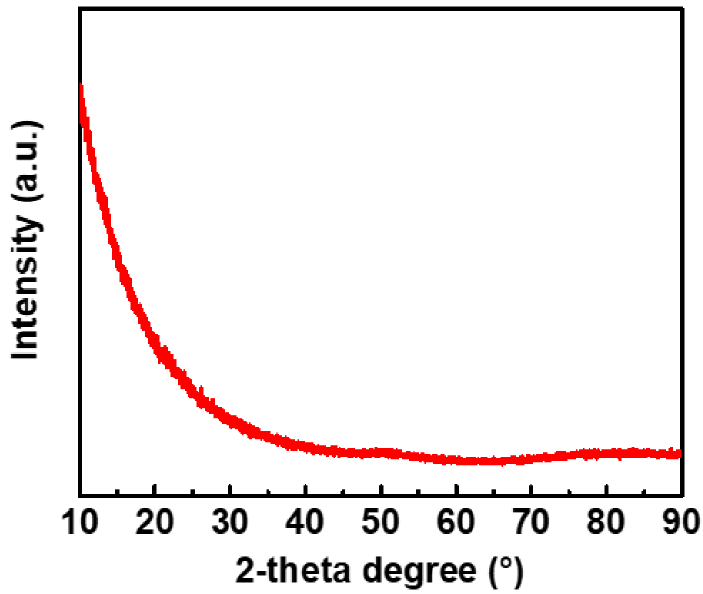

Fig. S13 Grazing incidence X-ray diffraction (GI-XRD) pattern of the Al_2O_3 nanolayers on a Si substrate.

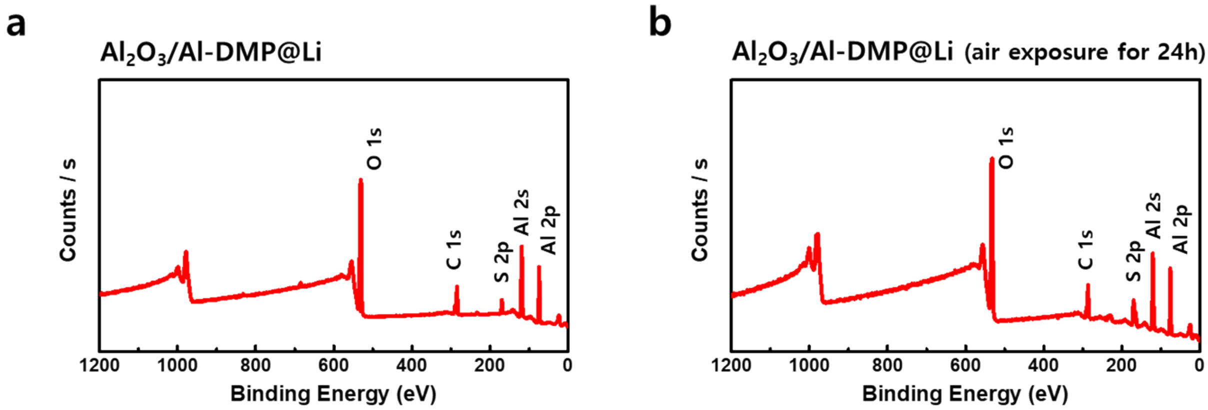

	Al_2O_3/Al-DMP@Li				
Element	Li	O	C	S	Al
Atomic %	0	50.86	10.38	6.47	32.29

	Al_2O_3/Al-DMP@Li (air exposure for 24h)				
Element	Li	O	C	S	Al
Atomic %	0	52.13	11.02	5.68	31.17

Fig. S14 XP spectra for the Al_2O_3/Al-DMP@Li (a) before air exposure, (b) after air exposure for 24h.

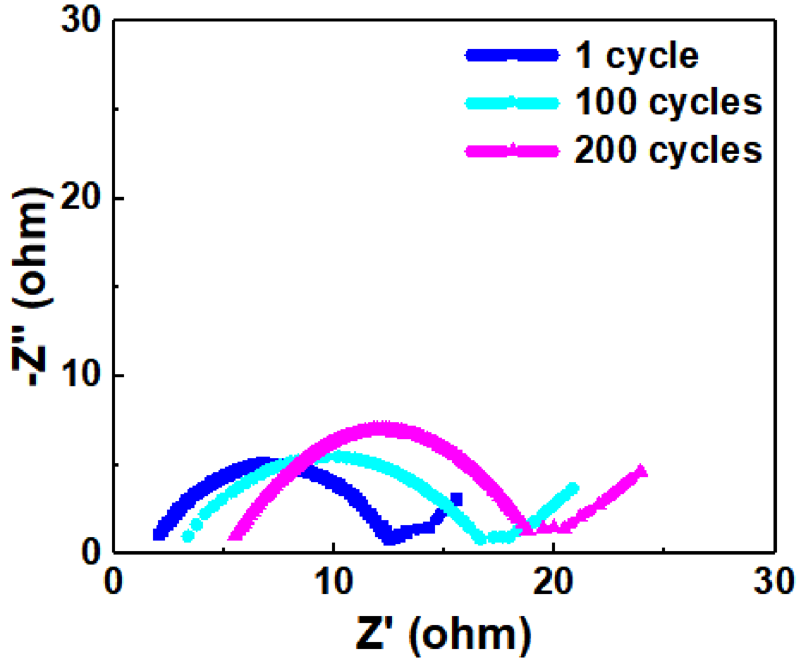

Fig. S15 The Nyquist plots of Al_2O_3/Al-DMP@Li symmetric cells after cycles.

	Al_2O_3/Al-DMP@Li
After 1 cycling (R_{SEI})	10.4
After 1 cycling (σ, $S\ cm^{-1}$)	$3.6x\ 10^{-7}$
After 200 cycling (R_{SEI})	13.2
After 200 cycling (σ, $S\ cm^{-1}$)	$2.4x\ 10^{-7}$

Table S4. Impedance results and calculated Li-ion conductivity of the Al_2O_3/Al-DMP superlattice after 1 cycle and after 200 cycles.

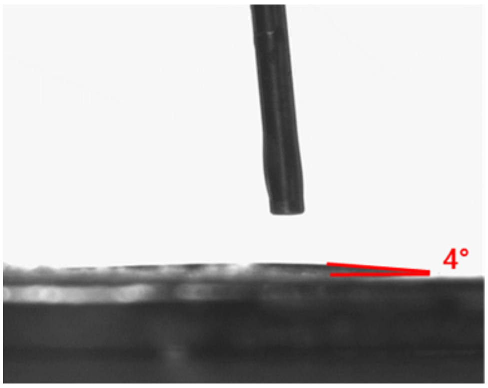

Fig. S16 Electrolyte droplet contact angle on Al_2O_3/Al-DMP@Li.

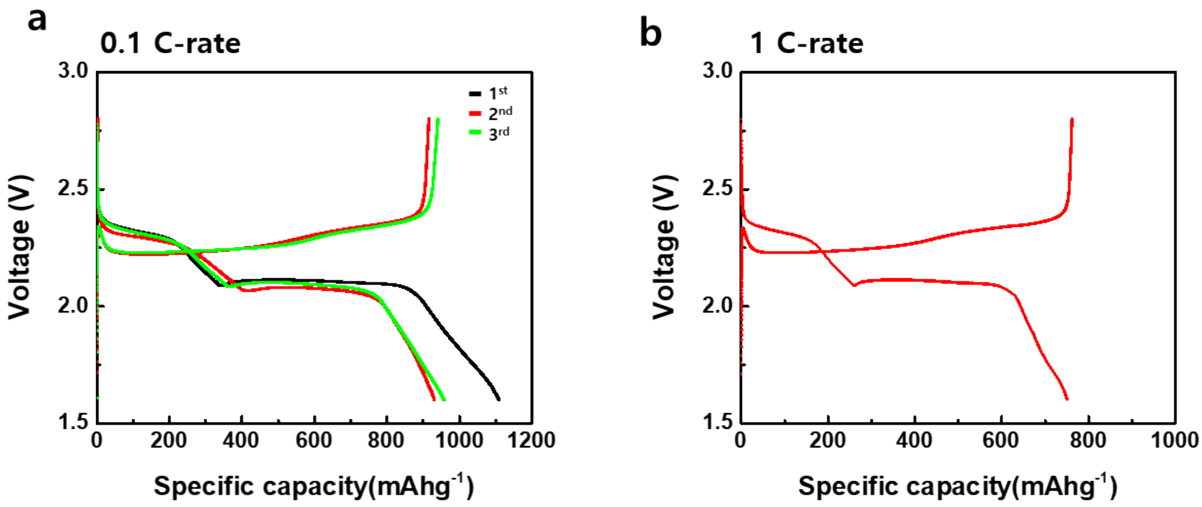

Fig. S17 Voltage profiles of full cells with Al_2O_3/Al-DMP@Li‖S/KB (a) at 0.1 C-rate, (b) the 1st charge/discharge at 1 C-rate.

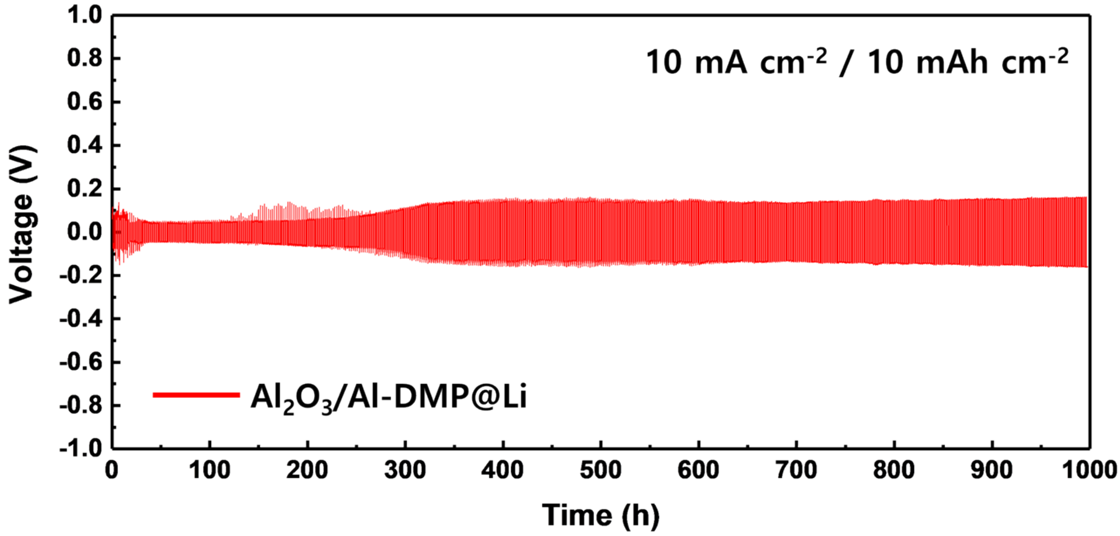

Fig. S18 Galvanostatic cycling performance of Al_2O_3/Al-DMP@Li symmetric cells at current density/areal capacity of 10 mA cm^{-2}/10 mAh cm^{-2} in 1 M LiTFSI in DOL/DME (1:1 by volume) with 2 wt % $LiNO_3$ exposed to air during 48 h at 25 °C and 50 % humidity.

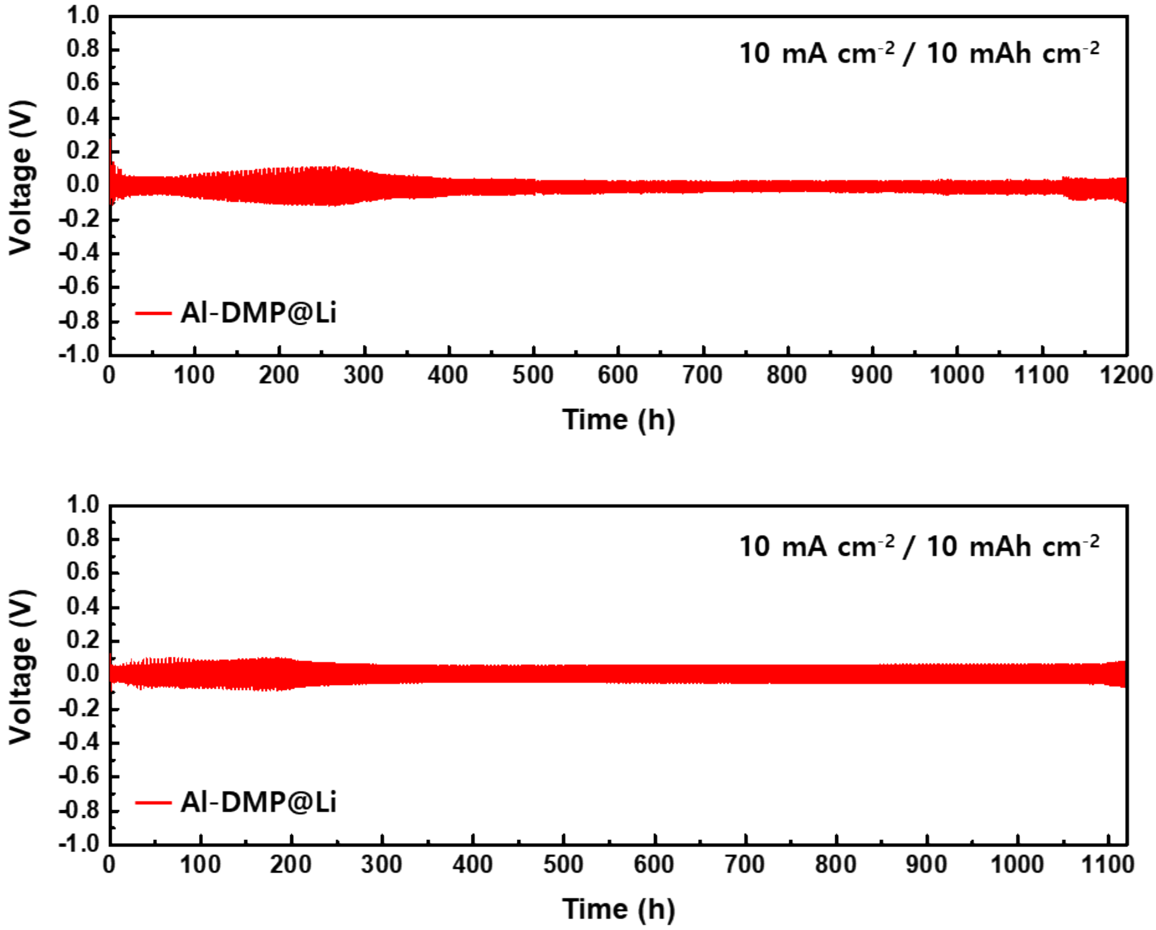

Fig. S19 Additional galvanostatic cycling performance data for Al-DMP@Li symmetric cells over 1000 cycles.

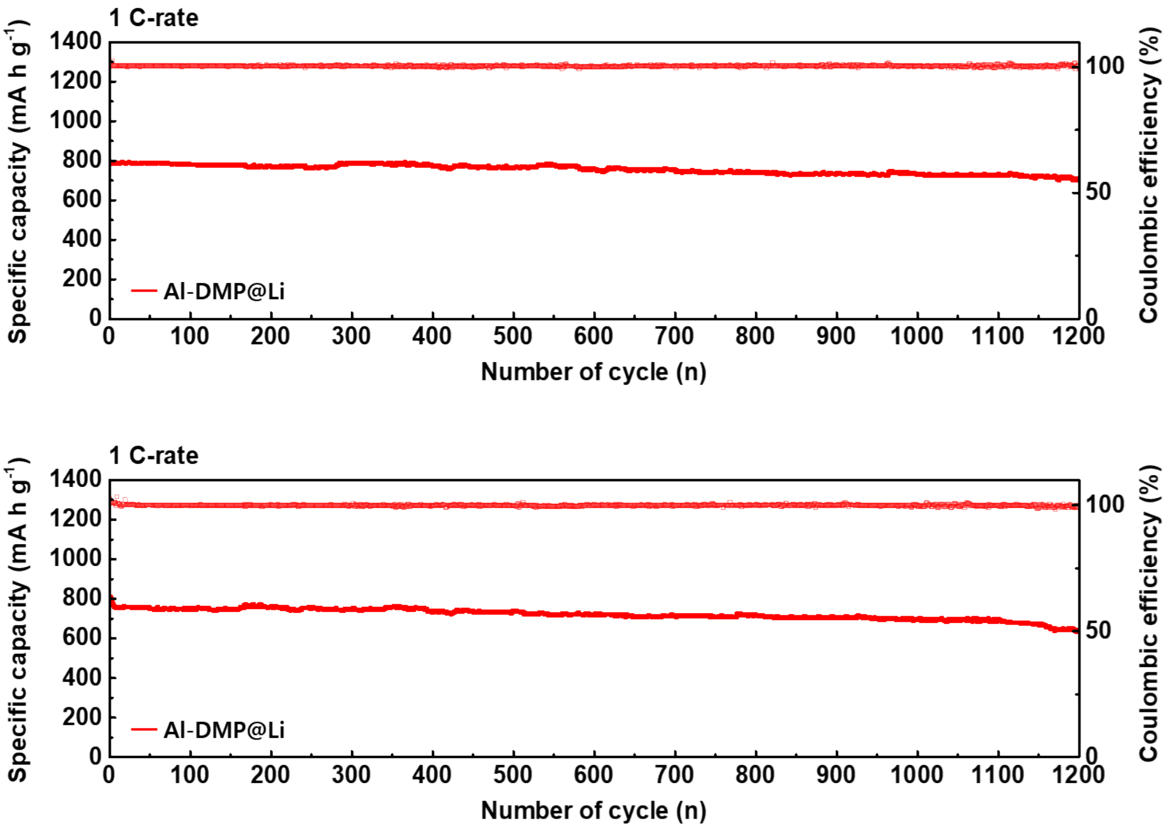

Fig. S20 Additional electrochemical performance data for Li-S full cells with Al-DMP@Li‖S/KB over 1100 cycles.

Table S5. Electrochemical performance comparison of Li||Li symmetric batteries coated by Al-DMP in this work and by other ALD, MLD films and other promising coatings.

	Process	Thickness (nm)	Electrolyte	Current density (mA cm^{-2})	Areal capacity (mAh cm^{-2})	Time (h)	Ref.
Al-DMP	MLD	50	1M LiTFSI in 1:1 DOL/DME with 2% $LiNO_3$	10	10	1000	This work
Al_2O_3	ALD	2-3	1M $LiPF_6$ in 1:1 EC/DMC	1	0.25	1259	1
Al_2O_3	ALD	~5	1M LiTFSI in 1:1 DOL/DME with 1% $LiNO_3$	5	1	75	2
Polyurea	MLD	~4	1M $LiPF_6$ in 1:1:1 EC/DEC/DMC	1	1	460	3
Alucone	MLD	5	1M LiTFSI in 1:1 DOL/DME with 1% $LiNO_3$	5	1	330	2
Zircone	MLD	~5	1M $LiPF_6$ in 1:1:1 EC/DEC/DMC	5	1	100	4
Gradient Zn/PU	MLD	~8	1M $LiPF_6$ in 1:1:1 EC/DEC/DMC	6	1	100	5
LiGL (lithicone)	MLD	~160	1M LiTFSI in 1:1 DOL/DME	7.5	1	940	6
Al_2O_3/Alucone	ALD/MLD	~30	1M LiTFSI in 1:1 DOL/DME	1	2	700	7
LiPEO–UPy	Drop-casting	~70	1M LiTFSI in 1:1 DOL/DME with 2% $LiNO_3$	5	10	1000	8
COF_{TpPa}	Drop-casting	170	1M LiTFSI in 1:1 DOL/DME	10	10	500	9
Li_2S/Li_2S_2-Array Li	Evaporation	16000	1M LiTFSI in 1:1 DOL/DME	10	10	250	10

Table S6. Comparison of the air stability of Li metal electrodes coated by Al2O3/Al-DMP in this work and by other ALD, MLD films and other promising coatings.

	Process	**Thickness (nm)**	**Air stability (h)**	**Ref.**
Al_2O_3/Al-DMP	ALD/MLD	54	60	This work
Zircone	MLD	~5	6	4
ZrO_2	ALD	190	10	11
Al_2O_3	ALD	36	20	12
Li_2Ga	Drop-casting	10000	24	13
Li-Wax-PEO	Dip-coating	30000	24	14
PVDF-HFP	Drop-casting	25000	48	15

References

1 E. Kazyak, K. N. Wood and N. P. Dasgupta, *Chem. Mater*., 2015, **27**, 6457–6462.

2 Y. Zhao, L. V. Goncharova, Q. Sun, X. Li, A. Lushington, B. Wang, R. Li, F. Dai, M. Cai and X. Sun, *Small methods*, 2018, **2**, 1700417.

3 Y. Sun, Y. Zhao, J. Wang, J. Liang, C. Wang, Q. Sun, X. Lin, K. R. Adair, J. Luo, D. Wang, R. Li, M. Cai, T.-K. Sham and X. Sun, *Adv. Mater*., 2019, **3**1, 1806541.

4 K. R. Adair, C. Zhao, M. N. Banis, Y. Zhao, R. Li, M. Cai and X. Sun, *Angew. Chem. Int. Ed*., 2019, **58**, 15797–1580.

5 Y. Sun, C. Zhao, K. R. Adair, Y. Zhao, L. V. Goncharova, J. Liang, C. Wang, J. Li, R. Li, M. Cai, T.-K. Sham and X. Sun, *Energy Environ. Sci*., 2021, **14**, 4085-4094.

6 X. Meng, K. C. Lau, H. Zhou, S. K. Ghosh, M. Benamara, and M. Zou, *Energy Mater. Adv*., 2021, **2021**, 9786201.

7 Y. Zhao, M. Amirmaleki, Q. Sun, C. Zhao, A. Codirenzi, L. V. Goncharova, C. Wang, K. Adair, X. Li, X. Yang, F. Zhao, R. Li, T. Filleter, M. Cai, and X. Sun, *Matter*, 2019, **1**, 1215-1231.

8 G. Wang, C. Chen, Y. Chen, X. Kang, C. Yang, F. Wang, Y. Liu and X. Xiong, *Angew. Chem. Int. Ed*., 2020, **59**, 2055–2060.

9 D. Chen, P. Liu, L. Zhong, S. Wang, M. Xiao, D. Han, S. Huang and Y. Meng, *Small,* 2021, **17**, 2101496.

10 J. Di, J.-L. Yang, H. Tian, P. Ren, Y. Deng, W. Tang, W. Yan, R. Liu and J. Ma, *Adv. Funct. Mater*., 2022, **32**, 2200474.

11 P. K Alaboina, S. Rodrigues, M. Rottmayer, S.-J. Cho, *ACS Appl. Mater. Interfaces*, 2018, **10**, 32801–32808.

12 A. C. Kozen, C.-F Lin, A. J. Pearse, M. A. Schroeder, X. Han, L. Hu, S.-B. Lee, G. W. Rubloff and M. Noked, *ACS Nano*, 2015, **9**, 5884–5892.

13 S. Liu, Q. Zhao, X. Zhang, J. Liu, L. Dai, L. Wanga and J. Luo, *J. Mater. Chem. A*, 2020, **8**, 17415-17419.

14 Y. Zhang, W. Lv, Z. Huang, G. Zhou, Y. Deng, J. Zhang, C. Zhang, B. Hao, Q. Qi, Y.-B. He, F. Kang and Q.-H. Yang, *Sci. Bull.*, 2019, **64**, 910-917.

15 Y. Xiao, R. Xu, C. Yan, Y. Liang, J.-F. Ding and J.-Q. Huang, *Sci. Bull.*, 2020, **65**, 909-916.